

Computer simulation of proton channelling in silicon

N K DEEPAK, K RAJASEKHARAN* and K NEELAKANDAN

Department of Physics, University of Calicut, Malappuram 673 635, India

*Department of Physics, Malabar Christian College, Kozhikode 673 001, India

MS received 11 October 1999; revised 12 June 2000

Abstract. The channelling of 3 MeV protons in the $\langle 110 \rangle$ direction of silicon has been simulated using Vineyard model taking into account thermally vibrating nuclei and energy loss due to ion-electron interactions. A beam made up of constant energy particles but with spatial divergence has been simulated for the purpose. The values of the minimum scattering yield and half width of the channelling dip are shown to be depth sensitive and agree well with the measured values. The dependence of yield on the angle of incidence has been found to give information of all three types of channelling. The critical angles for the three types of channelling and wavelength of planar oscillations are consistent with the previous calculations.

Keywords. Channelling; close collision yield; half-angle; minimum yield.

PACS No. 61.85

1. Introduction

When fast ions of MeV energy impinge on a crystal, they undergo a series of correlated collision with the lattice atoms. Some of them pass through the 'channels' in the crystal undeflected. This phenomenon called channelling finds widespread application in the field of crystallography, ion implantation, lattice location of impurity atoms and defects. As this phenomenon involves the interaction of fast moving ions with many atoms in the crystal, a rigorous and exact theoretical analysis of this complex many-body problem has met with only limited success. Therefore in the study of the phenomenon as well as its application, experiments are interpreted or closely supported by computer simulation techniques.

Over the years many computer models have been developed to simulate channelling. Early programmes were based on binary collision model [1]. Here an ion is assumed to interact with only the near atom. Results with this model are in general agreement with the measurements though significant discrepancies are seen in it. One of the shortcomings of the theory is that it does not consider the interaction of the ion with a large number of nuclei in the neighbouring rows and planes, although it is this aspect which leads to the characteristic features of channelling particularly planar and hyperchannelling. This model also does not allow for the determination of energy loss suffered by well-channelled ions and hence is not ideal for simulating planar and hyperchannelling.

Later Lindhard [2] introduced the continuum string approximation. Here the atomic rows are approximated by strings of uniformly smeared out positive charges in the direction of the channelling axis. This approximation is justified if the ion moves in a trajectory farther than a critical distance from the string and if the angle transverse to the channelling axis is less than a limiting angle. It is also well known that the changes in the ion-atom potential and field due to thermal vibration are appreciable only for distances less than 0.1 \AA [3, 4]. When close encounter processes are considered binary collision model is superior to continuum model.

Smulders and Boerma [5] tried to overcome the demerits of these two methods by combining the advantages of both by considering the interaction with the nearest atom using binary collision model and with the surrounding atomic rows using continuum approximation model. In this process for the nearest atomic row, interaction with only the nearest atom is considered, neglecting the effect of other atoms. This results in an underestimation of total transverse field.

To overcome all these problems we here introduce the ion-many nuclei interaction throughout the crystal. In this model the field at any point is obtained by considering the ion-atom interaction using an appropriate binary potential, with each of the neighbouring atoms in the crystal. This procedure thus takes care of both close collisions processes as well as distant processes. Concept of such a model, called Vineyard model or N -body model [6] is not new. The major problem with this model is that a large computation time is involved. Hence it has not found any serious application so far. But with the recent availability of high-speed computers we decided to test the efficacy of the model. The main attraction in pursuit of this model is that the model simulates the real physical situation as close as possible.

2. Theory

2.1 Beam divergence

A channelling experiment involves bombarding a single crystal target with a beam of high energetic ions. The well-collimated beam is incident on the crystal at a small angle ψ_0 with respect to the normal to the surface; the crystal itself is cut with the normal along a crystal axis, called the channelling axis. If the angle of incidence is less than a certain critical angle, the ion is channelled within the crystal [7]. The plane containing the incident direction and the normal to the surface, may subtend an angle θ_0 with a major crystal axis. This angle is defined as the azimuthal angle (see figure 1) and is measured in the anti-clockwise direction.

To study the dependence of the yield from the close ion-nuclei interactions on the angle ψ_0 , the detector is positioned at a wide angle to the direction of incidence. The yield is then measured by varying ψ_0 .

To simulate channelling effects in a computer one normally invokes the particle trajectory approximation [8]. In this method the path followed by a sample of incident ions in the crystal is determined. To select a typical sample of the beam, we consider a unit cell in the plane transverse to the channelling axis. A large number of points are randomly chosen inside the cell and they are treated as the points of incidence of the ions in the beam.

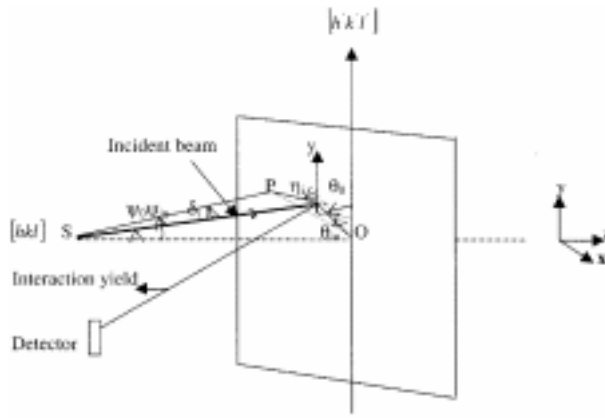


Figure 1. Schematic diagram of an experimental arrangement for channelling to study close interaction processes. SP is the trajectory of a typical particle emitted from source S at an angle δ_i off the average direction SC. The momentum vector transverse to the average direction is along line PC.

The position co-ordinates of the points chosen define the initial position co-ordinates of the ions.

If E is the energy of an ion, its velocity v is given by the equation

$$v = \sqrt{\frac{2E}{M_1}}, \quad (1)$$

where M_1 is the mass of the incident ion. Defining a co-ordinate system with the z -axis along the channelling axis, the component of velocity along this axis is

$$v_z = v \cos \psi_{in}, \quad (2)$$

where ψ_{in} is the angle of incidence of the ion. Here it is assumed that however well a beam is collimated, it will have a small spatial divergence with the result that an ion can have an angle of incidence ψ_{in} different from the mean angle ψ_0 . The velocity component transverse to the z -axis is

$$v_{\perp} = v \sin \psi_{in}. \quad (3)$$

Due to divergence the azimuthal angle for an ion θ_{in} can also be different from the mean azimuthal angle θ_0 . Defining the y -axis to be along the reference axis in the plane of the crystal surface and x -axis perpendicular to it, the velocity components in the transverse plane are

$$v_x = -v_{\perp} \sin \theta_{in} \quad (4)$$

and

$$v_y = v_{\perp} \cos \theta_{in}. \quad (5)$$

Due to beam divergence a large number of ions make small angles δ_i s with respect to the average beam direction and azimuthal angles η_i s in the plane transverse to the average

direction SC as in figure 1. δ_i s and η_i s take on random values with the former following a Gaussian distribution with a variance Δ centred about zero degree and the latter following a rectangular distribution between 0° and 360° . Then from the geometry it can be seen that the ions in the beam will have different ψ_{in} s and θ_{in} s related to their characteristic angles δ_i s and η_i s given by the equations

$$\cos \psi_{in} = \cos \psi_0 \cos \delta_i - \sin \psi_0 \sin \delta_i \cos \eta_i \quad (6)$$

and

$$\theta_{in} = \theta_0 + \theta', \quad (7)$$

where θ' is given by

$$\tan \theta' = \left(\frac{\tan \delta_i \sin \eta_i}{\cos \psi_0 (\tan \psi_0 + \tan \delta_i \cos \eta_i)} \right). \quad (8)$$

2.2 Vineyard model

The force on an ion at any point \mathbf{r} in the crystal is given by the equation

$$M_1 \frac{d^2 \mathbf{r}}{dt^2} = - \left[\frac{\partial V(\mathbf{r})}{\partial x} \mathbf{i} + \frac{\partial V(\mathbf{r})}{\partial y} \mathbf{j} + \frac{\partial V(\mathbf{r})}{\partial z} \mathbf{k} \right]. \quad (9)$$

The position vector \mathbf{r} is given by

$$\mathbf{r} = x\mathbf{i} + y\mathbf{j} + z\mathbf{k}, \quad (10)$$

where (x, y, z) is the position co-ordinate of the ion. \mathbf{i} , \mathbf{j} and \mathbf{k} are unit vectors along the x , y and z axes respectively. In the Vineyard model the potential $V(\mathbf{r})$ is given by the sum of the electrostatic Coulombic potentials due to all the nuclei in the crystal. The effect of electrons is taken into account by the use of appropriate screening function. Thus $V(\mathbf{r})$ may be written as

$$V(\mathbf{r}) = \sum_{i=1}^N V_s(\mathbf{r}, \mathbf{r}_i) \quad (11)$$

where N is the total number of atoms in the crystal and V_s , the potential due to a single nucleus at \mathbf{r}_i is

$$V_s(\mathbf{r}, \mathbf{r}_i) = \frac{Z_1 Z_2 e^2}{4\pi\epsilon_0 |\mathbf{r} - \mathbf{r}_i|} \xi \left(\frac{|\mathbf{r} - \mathbf{r}_i|}{a_T} \right). \quad (12)$$

The screening function ξ is given by Lindhard [9]

$$\xi \left(\frac{|\mathbf{r} - \mathbf{r}_i|}{a_T} \right) = 1 - \left[1 + \left(\frac{3a_T^2}{|\mathbf{r} - \mathbf{r}_i|^2} \right) \right]^{-\frac{1}{2}}. \quad (13)$$

a_T is the screening radius given by

$$a_T = 0.8853 a_0 Z_2^{-1/3}, \quad (14)$$

where $a_0 = 0.528 \text{ \AA}$ is the Bohr radius. Z_1 and Z_2 are the atomic numbers of the incident ion and the target atom respectively, e being the electronic charge.

2.3 Thermal vibration

In writing the expression (11) for Coulombic potential one assumes a static nucleus. Due to thermal energy the nuclei in the target oscillates about the equilibrium points \mathbf{r}_i . Hence at any instant the nuclei may be found slightly displaced to a point \mathbf{r}'_i , so that the instantaneous field $F_i(\mathbf{r})$ at \mathbf{r} due to a nucleus at \mathbf{r}_i is given by

$$F_i(\mathbf{r}, \mathbf{r}_i, \mathbf{r}'_i, T) = -f(\mathbf{r}_i, \mathbf{r}'_i) \left[\frac{\partial V_s(\mathbf{r}, \mathbf{r}'_i)}{\partial \mathbf{r}} \right], \quad (15)$$

where $f(\mathbf{r}_i, \mathbf{r}'_i)$ is the probability that the nucleus centred at \mathbf{r}_i is displaced to \mathbf{r}'_i , and is expressed as a Gaussian probability function

$$f(\mathbf{r}_i, \mathbf{r}'_i) = \frac{1}{\sqrt{2\pi u_1^2}} \left[\exp \left(\frac{-|\mathbf{r}_i - \mathbf{r}'_i|^2}{2u_1^2} \right) \right], \quad (16)$$

where u_1^2 is the mean-square displacement of the nucleus in any direction. Its value as given by the Debye temperature of the target and T is its absolute temperature.

To take into account the effect of the oscillations of all nuclei in the crystal we adopt an averaging procedure given by Andersen and Feldman [10]. Accordingly the average field at \mathbf{r} due to a nucleus centred at \mathbf{r}_i is given as

$$\langle F(\mathbf{r}, \mathbf{r}_i, T) \rangle = \int_{-\infty}^{+\infty} F_i(\mathbf{r}, \mathbf{r}_i, \mathbf{r}'_i, T) d\mathbf{r}'_i. \quad (17)$$

2.4 Energy loss

Ions of a few MeV energies lose energy as they traverse through a crystal mainly by inelastic scattering with the electrons. When the ions are channelled, there is a significant reduction in the energy loss as they encounter more valence electrons than core electrons. As a result the energy loss suffered by the ions become position dependent. Among the various theories on determining this anisotropic energy loss, we adopt the method followed by Bontemps and Fontinille [11,4].

It gives reasonably good estimate of energy loss and is also very easy to use. The loss of energy for an ion is in effect a retarding force on the ion in the direction of penetration. Therefore this rate of loss of energy should be considered as an additional force in the z direction when equation (9) is considered.

2.5 Close-encounter probability

With known initial position and velocity co-ordinates, the equations of motion are integrated to obtain the ion trajectories in the crystal up to any desired depth. The close-encounter probability $P(x, y)$ is calculated from the distribution of atoms inside a channel using the expression [12]

$$P(x, y) = \frac{\cos \psi}{(2\pi u_1^2)} \sum_{i=1}^n \exp \left[\frac{-\left((x - x_i)^2 + (y - y_i)^2\right)}{2u_1^2} \right], \quad (18)$$

where (x_i, y_i) is the position of the i th atom in the transverse plane.

If $n(x, y, z)$ is the number of ions in the element ds of the transverse plane at depth z , the close-encounter yield $\chi(z)$ at z is obtained by integrating $P(x, y) n(x, y, z)$ over the entire area of the transverse plane. Thus

$$\chi(z) = \int_s P(x, y) n(x, y, z) ds. \quad (19)$$

The total yield χ_{tot} within a depth D , from close encounter process is given by the integral

$$\chi_{\text{tot}} = K \int_0^D \chi(z) dz, \quad (20)$$

where K is a normalization constant.

3. Calculation

To implement the model we simulate the proton channelling in the $\langle 110 \rangle$ direction of a single crystal of silicon.

A program BEAM simulates a beam made up of large number of protons, typically 1000. For this a standard random number generating 'library function' is made use of to generate the position co-ordinate of the points of incidence of protons in a unit cell. A unit cell is the smallest unit on the surface of the crystal, which by translation operations can generate the entire crystal plane. Figure 2 shows the plane transverse to the $\langle 110 \rangle$ axis with the unit cell.

To generate the characteristic angles δ_i s and η_i s, normal random variables ζ_i s with mean zero and variance one are drawn by a method based on central limit theorem [13]. If Δ is the desired divergence of the beam, then the values of δ_i s are given by the equation

$$\delta_i = |\zeta_i \Delta|. \quad (21)$$

A set of random numbers with a rectangular distribution is then generated by using the library function and they are multiplied by 2π so that the products η_i s are uniformly distributed between 0 and 2π .

With the values of δ_i and η_i the angles ψ_{in} and θ_{in} and hence the initial velocity coordinates are determined by eqs (6), (7), (2), (4) and (5). All protons are assumed to be incident on the crystal with the same energy 3 MeV. The data made up of the initial spatial and velocity co-ordinates of 1000 protons is then the simulated beam.

A program TRAJ uses this data to numerically integrate the force eq. (9) to obtain the trajectories of all the protons in the crystal. For this the numerical integration is started by Runge-Kutta method [14]. To save precious computer time summation in eq. (11) is limited to only those neighbouring atoms that comes within a certain distance. To obtain this cut-off distance, the field at a point in the mid-channel axis was evaluated by progressively increasing the number of neighbouring atoms considered. It was then found that

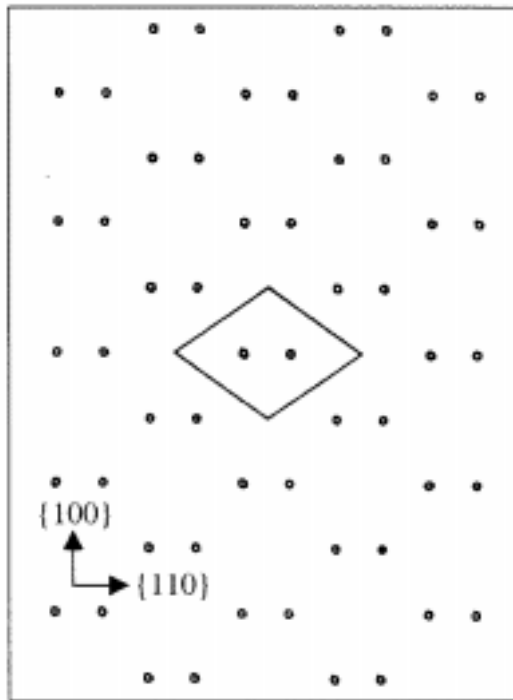


Figure 2. Shows the plane transverse to the $\langle 110 \rangle$ direction of silicon. Dots represent string of atoms and rhombus is the unit cell.

the contribution to the total field from atoms beyond a distance of 3 \AA was less than one percentage of the total. Therefore when field is evaluated only those atoms that comes within a distance of 3 \AA from the ion is considered for the summation in eq. (11). The integration involved in eq. (17) is time consuming and is prohibitive to evaluate in real time. But calculation [4] shows that thermal effects become significant only when an ion comes closer than 0.1 \AA from a nucleus. So we choose a cubic grid of $20 \times 20 \times 20$ points within a square of size 0.2 \AA centred about a nucleus. The field at these points are evaluated by eq. (17) and stored in a data file. If the ions happen to be within this square, field at the point was approximated to the field at the nearest point in the grid.

With the starting values thus obtained, the trajectory evaluation is continued by Adams–Bashforth–Moulton predictor–corrector formula [15]. Computations have been performed up to a depth of 8000 \AA . The result is output in a data file as position co-ordinates of the ions at regular depth intervals of 2 \AA .

A program YIELD uses these co-ordinates to determine $\chi(z)$ at regular intervals of 2 \AA using eq. (19). These values are then added to obtain the total yield. The protons in the beam are divided into groups of 250 particles and YIELD computes $\chi(z)$ and χ_{tot} for each group from which the mean and standard deviation of $\chi(z)$ and χ_{tot} are determined.

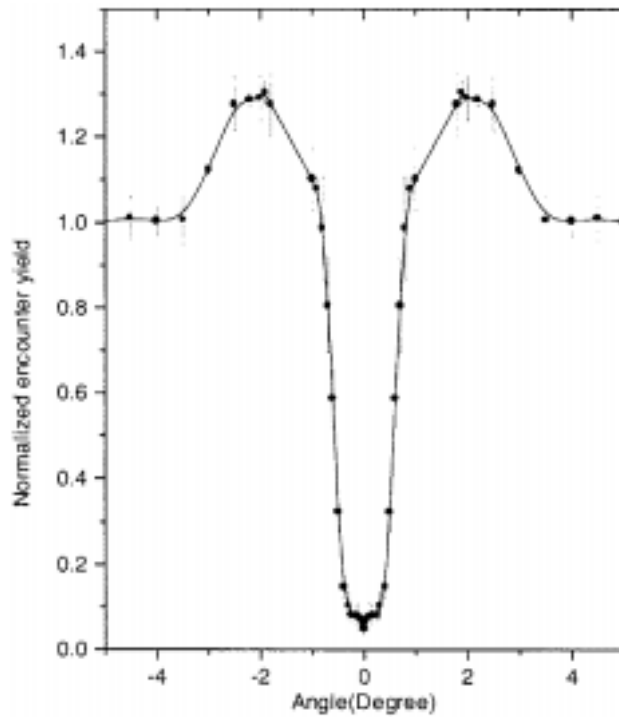


Figure 3. Axial channelling dip for 3 MeV protons incident along $\langle 110 \rangle$ direction of silicon. Beam divergence is 0.001° . Solid line is drawn to aid the eye.

4. Results and discussion

Figure 3 shows the variation of yield with ψ_0 for an azimuthal angle $\theta_0 = 0^\circ$ and beam divergence of 0.001° . The crystal temperature was chosen as 293°K . The error bars shown are the standard deviations for each mean value.

The values of yield at various ψ_0 are indicative of the different classes of trajectories inside the crystal. The dip centred about 0° is a result of most of the particles in the beam undergoing axial channelling. This significantly reduces the chance of ion–nucleus close encounter. The flattening of the yield at higher angles is due to most particles moving randomly in the crystal. The graph is drawn by normalizing the random values to unity. The two shoulder-like peaks on either side of the dip are due to a large number of quasi-channelled ions where ions frequently change from axial channelled to random and viceversa. Such particles spend relatively more time around the rows of atoms, thus increasing the chances of close interaction processes.

Channelling is usually characterized by specifying the minimum yield χ_{\min} and the half width of the dip $\psi_{1/2}$ at $\chi_{1/2}$ defined as $\chi_{1/2} = 1/2(1 + \chi_{\min})$. χ_{\min} and $\psi_{1/2}$ are depth dependent. When no depth is specified the reported values of $\psi_{1/2}$ and χ_{\min} are taken to be the values at the surface obtained by extrapolating to zero depth.

Figures 4 and 5 shows the variations of χ_{\min} and $\psi_{1/2}$ with depth. Solid line is shown

to aid the eye. Extrapolation to zero depth gives the surface values of χ_{\min} and $\psi_{1/2}$ as $0.038, 0.66^\circ$ respectively. It is seen that χ_{\min} value is higher than the experimental value of Davies *et al* [16] but much less than Feldman and Erginsoy [17] (see table 1). Considering the facts that χ_{\min} measurement is sensitive to depth (figure 4) and beam divergence (table 2) it may be concluded that the value we have obtained is good. Our value of $\psi_{1/2}$ is much higher than both experimental values. A probable explanation for this discrepancy can be seen in figure 5, which shows that $\psi_{1/2}$ value is also highly depth sensitive. Davies *et al* have reported that their surface values were measured in the range 0 to 8000 Å. From our figure it can be seen that at depth 8000 Å $\psi_{1/2}$ values agree very well with the measurements of Davies *et al*.

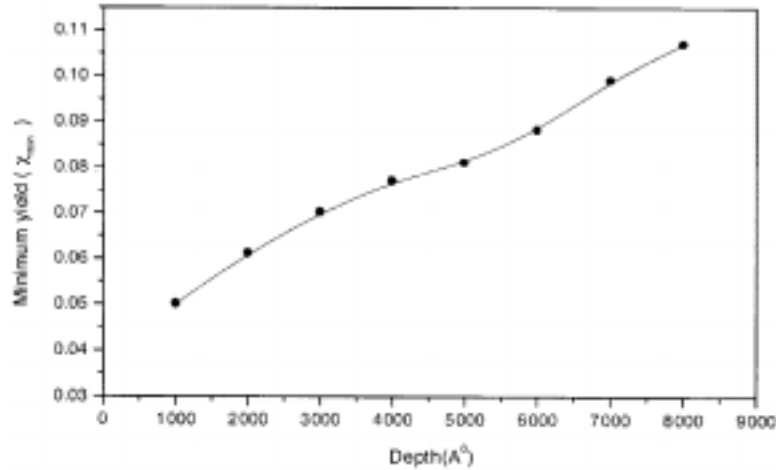


Figure 4. Variation of minimum yield with depth for a beam divergence of 0.001° .

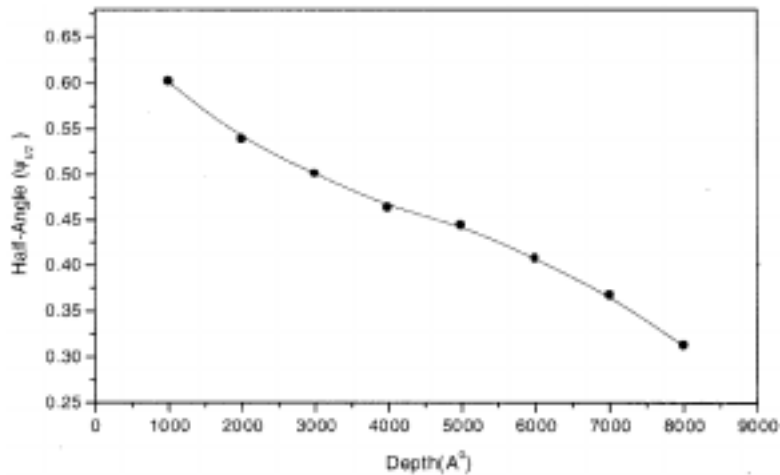


Figure 5. Variation of half-angle with depth for a beam divergence of 0.001° .

Table 1. Comparison with other results.

	Our value	Calculation of Barrett	Measurements of	
			Davies <i>et al</i> [16]	Feldman and Erginsoy [7]
$\psi_{1/2}$	0.66°	0.3°	0.26° ± 0.07°	0.22°
χ_{\min}	0.038	–	0.028 ± 0.003	0.073

Table 2. Computed values show the variations of minimum yield and half-angle for a depth of 1000 Å for various azimuthal angles and beam divergences.

	Beam divergence (azimuthal angle = 0°)		Azimuthal angle (beam divergence = 0.001°)		
	0°	0.001°	0.01°	45°	90°
$\psi_{1/2}$	0.582°	0.601°	0.616°	1.022°	0.597°
χ_{\min}	0.054	0.050	0.048	0.023	0.080

We repeated our calculation by varying θ_0 and beam divergence. Table 2 shows the variation of χ_{\min} and $\psi_{1/2}$ at 1000 Å. Considering the dependence of χ_{\min} and $\psi_{1/2}$ on all these factors it is clear that our computed values agree very well with the observed values. The values given by Barrett’s calculation themselves are based on computations performed up to 5000 Å.

The present calculation shows a structure around the minimum that is not seen in any experimental or simulation results. Figure 6 shows this portion of the curve magnified. It can be seen that the structure is a result of two close sharp peaks. The first peak occurs at 0.013° and the second peak at 0.158°. The innermost dip at 0° may be attributed to hyper-channelled particles, which are particles that are trapped by 12 neighbour rows of nuclei as they penetrate into the crystal. As in the case of axial channelling it may be said that the sharp peaks on either side of the dip are due to quasi-hyper channelled particles. The calculation of Lindhard [2] showed that the critical angle for hyper-channelling in the (001) direction of copper is 0.0125° which is close to the occurrence of our first peak.

The next dip may similarly be attributed to the planar-channelled particles where the particles are confined between two {110} planes and the peak to quasi-planar channelled particles. The critical angle for planar-channelled ions as given by the formula $\psi_a \approx 0.545 (nZ_1 Z_2 a/E)^{1/2}$ [7] gives a value of 0.16° for 3 MeV protons. It can be seen that this value is very close to the position of our second peak 0.158°.

Figure 7 shows the variation of yield with depth for protons incident with $\psi_0 = 0.08^\circ$. This angle falls within the dip due to planar-channelled particles. Therefore most of the ions executes an oscillation between the {110} planes as they penetrate the crystal. The occurrence of peaks in figure 7 should then correspond to the approach of many ions close to the atomic planes. If the oscillations are characterized by a wavelength λ then successive peaks should occur at $\lambda/2, 3\lambda/2$, etc and minima at $\lambda/4, 3\lambda/4 \dots$. Van Vliet [18] has derived a simple analytical expression for the wavelength

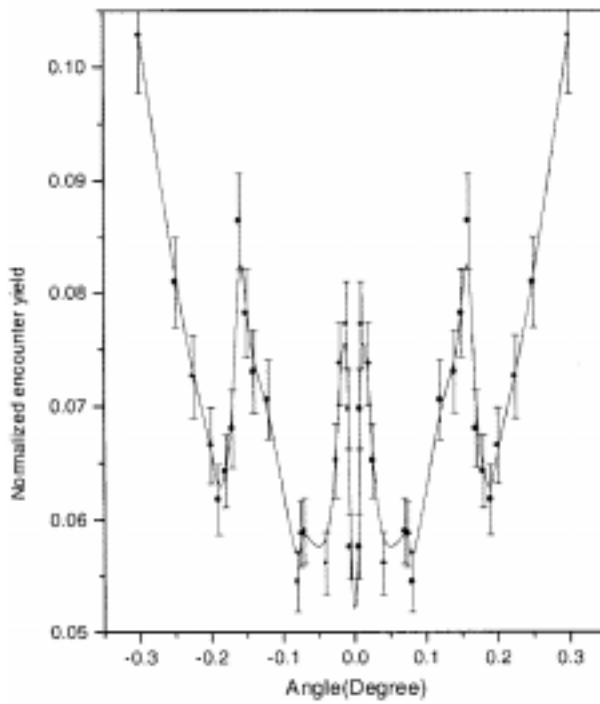


Figure 6. Computed planar and hyper channelling dips for 3 MeV ions incident along $\langle 110 \rangle$ direction of silicon.

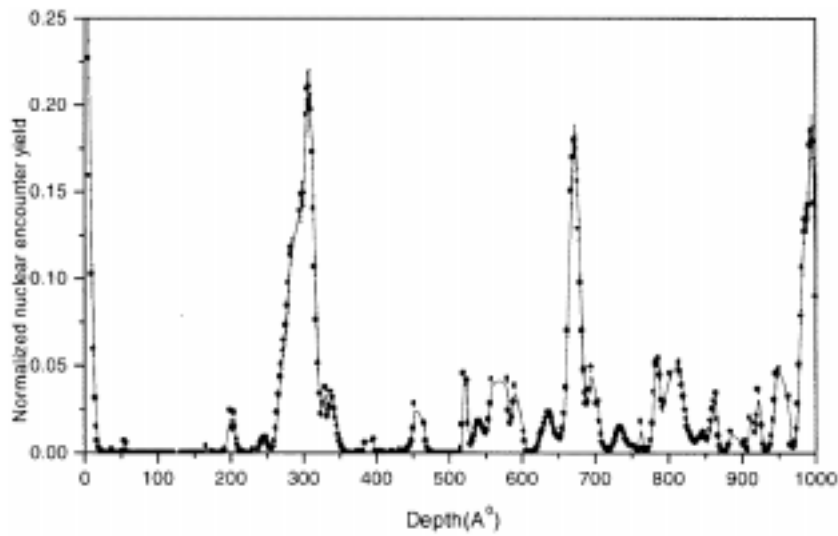


Figure 7. Shows the variation of nuclear encounter probability with depth for $\psi_0 = 0.08^\circ$. Beam divergence = 0.001° .

$$\frac{\lambda}{2} = \left(\frac{\pi}{2}\right) \frac{d_p}{\phi_r}, \quad (22)$$

where ϕ_r is given by

$$E\phi_r^2 = 2\pi a(Nd_p)Z_1Z_2e^2. \quad (23)$$

For the system in figure 7 this yields a value of $\lambda/2 \cong 325 \text{ \AA}$ in fair agreement with the computed value.

5. Conclusion

This paper reports an indigenously developed computer code for channelling of fast ions in crystals using Vineyard model and screened binary Coulombic potential. The paper reports for the first time the effect of all the three types of channelling in the close encounter yield. The values of half-angle and minimum yield also show excellent agreement with measurements, good enough to give crystal thickness. The success in simulating all the three basic types of channelling and the excellent predictions of $\psi_{1/2}$ and χ_{\min} values can be attributed to the superiority of our model in simulating the close ion–nucleus interaction as well as the distant ion–many nuclei interactions.

References

- [1] J H Barrett, *Phys. Rev.* **166**, 219 (1968)
- [2] J Lindhard, *K. Dan. Vidensk. Mat. Fys. Medd.* **14**, 34 (1965)
- [3] B R Appleton, C Erginsoy and W M Gibson, *Phys. Rev.* **161**, 330 (1967)
- [4] K Rajasekharan and K Neelakandan, *Pramana – J. Phys.* **31**, 399 (1988)
- [5] P J M Smulders and D O Boerma, *Nucl. Instrum. Methods* **B29**, 471 (1987)
- [6] D V Morgan, *Channelling: Theory, observation and applications* (John Wiley and Sons, 1973)
- [7] Donald S Gemell, *Rev. Mod. Phys.* **46**, 129 (1974)
- [8] J A Ellison, S T Chui and W M Gibson, *Phys. Rev.* **B18**, 5963 (1978)
- [9] J Lindhard, V Nielsen and M Sharff, *K. Dan. Vid. Selk. Mat.- Fys. Medd.* **36**, 10 (1968)
- [10] J U Andersen and L C Feldman, *Phys. Rev.* **B1**, 2063 (1970)
- [11] A Bontemps and J Fontinille, *Phys. Rev.* **B18**, 5963 (1978)
- [12] J H Barrett, *Phys. Rev.* **B3**, 1527 (1971)
- [13] J M Hammersley and D C Handscomb, *Monte Carlo methods* (Chapman and Hall, London, 1964)
- [14] J B Scarborough, *Numerical mathematical analysis* (Calcutta: Oxford and IBH, 1971)
- [15] K E Atkinson, *Elementary numerical analysis* (John Wiley and Sons, New York, 1985)
- [16] J A Davies, J Denhartog and J L Whitton, *Phys. Rev.* **165**, 345 (1968)
- [17] L Feldman and C Erginsoy, *Bull. Am. Phys. Soc.* **12**, 391 (1967)
- [18] D Van Vliet, *Radiation effects in solids* (Gordon and Breach, New York, 1973)